Angewandte Chemie
Eine Zeitschrift der Gesellschaft Deutscher Chemiker

Supporting Information

69451 Weinheim, Germany

Discovery of Small Molecules that Bind to K-Ras and Inhibit Sos-Mediated Activation**

*Qi Sun, Jason P. Burke, Jason Phan, Michael C. Burns, Edward T. Olejniczak, Alex G. Waterson, Taekyu Lee, Olivia W. Rossanese, and Stephen W. Fesik**

anie_201201358_sm_miscellaneous_information.pdf

Table of Contents

Supplementary Figure 1. Effect of compound **12** on Sos-mediated K-Ras activation. Comparison of intrinsic (black) and Sos-catalyzed nucleotide exchange in the absence (blue) or presence of increasing concentration of compound **12**. Exchange assays were performed by addition 1 μM K-Ras (G12D) to a mixture containing 1 μM Sos, 1 μM BODIPY-GTP, and 250 μM (orange), 500 μM (green), or 1 mM (red), respectively.

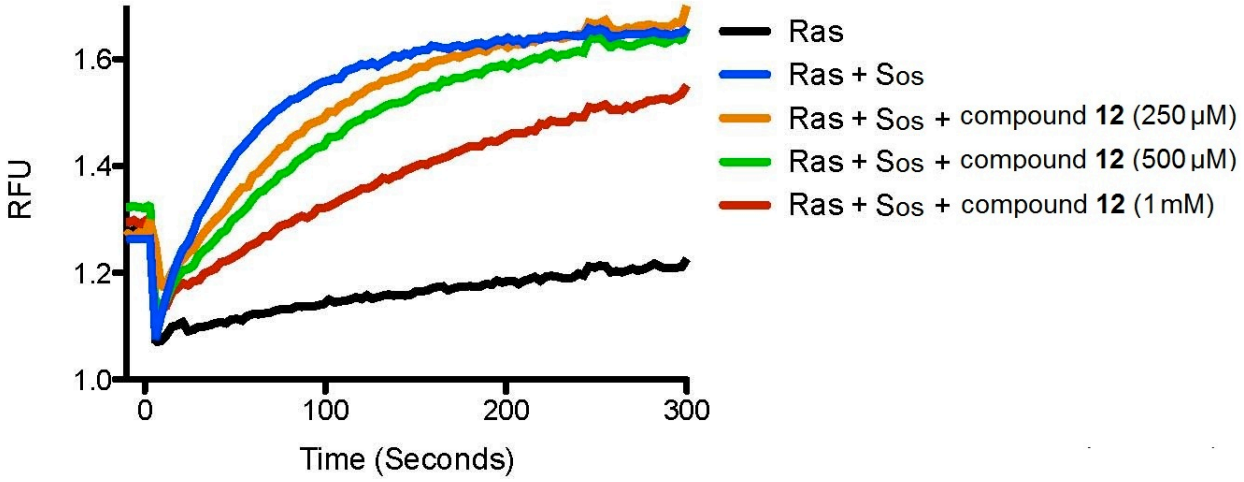

Supplementary Figure 2. ^{1}H-^{15}N HSQC spectra of uniformly ^{15}N-labeled GDP-bound K-Ras (G12D) with and without Sos and compound 13. A). [U-^{15}N] K-Ras (50 μM). B). [U-^{15}N] K-Ras (50 μM) / Sos (200 μM). C). [U-^{15}N] K-Ras (50 μM) / Sos (200 μM) / Compound **13** (4 mM). D). [U-^{15}N] K-Ras (50 μM) / Compound **13** (1 mM). Addition of an excess of Sos causes K-Ras resonance peaks to shift, broaden, and disappear when compared to K-Ras alone (A *vs*. B). Addition of compound **13** to the K-Ras/Sos complex causes peaks to reappear (C) which results in a spectrum similar to that obtained for the K-Ras/Compound **13** complex (D).

A. [U-^{15}N] K-Ras

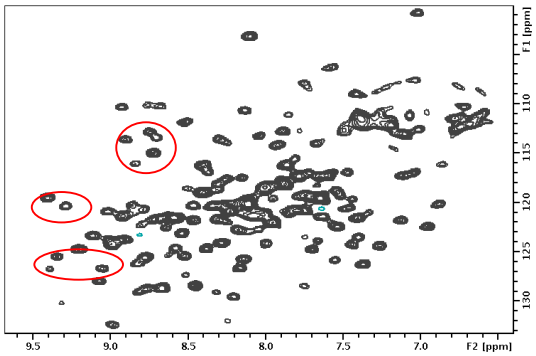

B. [U-^{15}N] K-Ras / Sos

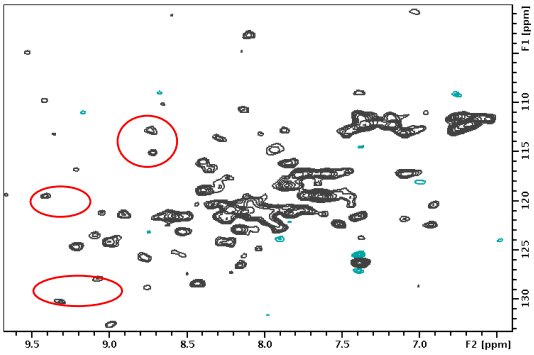

C. [U-^{15}N] K-Ras / Sos / Compound **13**

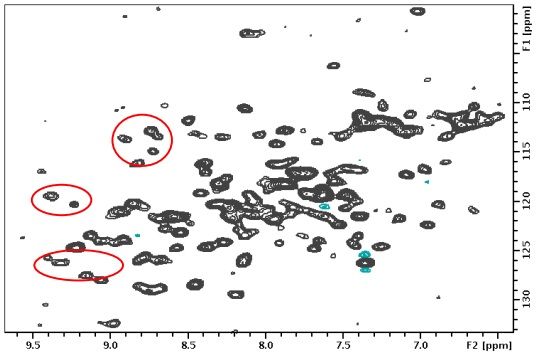

D. [U-^{15}N] K-Ras / Compound **13**

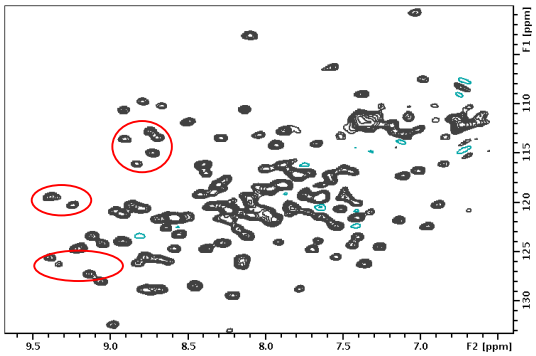

Supplementary Table 1. **X-ray data collection and refinement statistics.** Last resolution shell numbers are in parentheses.

	GDP K-Ras	GDP K-Ras/**2**	GDP K-Ras/**4**	GDP K-Ras/**5**
PDB entry	4EPR	4EPT	4EPV	4EPW
Data collection				
Space group	H 3 2	P 63	P 21 21 21	P 21 21 21
Cell dimensions				
a, b, c (Å)	94.36, 94.36, 122.36	93.06, 93.06, 37.20	39.14, 41.07, 91.96	39.22, 41.92, 91.45
α, β, γ (°)	90.00, 90.00, 120.00	90.00, 90.00, 120.00	90.00, 90.00, 90.00	90.00, 90.00, 90.00
Resolution (Å)	50.00 – 2.00 (2.03 – 2.00)	50.00 – 2.00 (2.03 – 2.00)	45.98 – 1.35 (1.37 – 1.35)	45.72 – 1.70 (1.73 – 1.70)
R_{merge}	11.8 (39.9)	11.3 (28.1)	9.2 (20.0)	10.6 (15.1)
$I / \sigma I$	17.4 (3.4)	10.2 (4.1)	14.2 (4.1)	8.6 (4.3)
Completeness (%)	99.9 (90.0)	99.5 (99.7)	96.9 (72.4)	94.4 (83.8)
Redundancy	8.7 (5.9)	4.7 (2.8)	4.1 (2.2)	2.9 (1.8)
Structure Refinement				
No. reflections	13572	11632	30436	15325
R_{work} / R_{free}	20.02 / 25.30	22.93 / 27.44	16.39 / 19.39	18.56 / 24.00
No. atoms				
Protein	1328	1323	1355	1355
GDP / Mg	28 / 1	28 / 1	28 / 1	28 / 1
Water	133	116	236	162
Ligand		14	19	18
B-factors				
Protein	26.86	20.00	12.16	16.27
GDP / Mg	19.03 / 25.18	12.95 / 10.0	11.92 / 10.51	18.14 / 14.62
Water	32.76	25.56	23.71	25.15
Ligand		16.46	17.70	15.22
R.m.s. deviations				
Bond lengths (Å)	0.027	0.024	0.029	0.026
Bond angles (°)	2.048	2.024	2.354	2.078

(Continued on next page)

Supplementary Table 1. (Continued)

	GDP K-Ras/**6**	GDP K-Ras/**13**
PDB entry	4EPX	4EPY
Data collection		
Space group	P 21 21 21	P 21 21 21
Cell dimensions		
a, b, c (Å)	39.13, 41.47, 91.73	38.98, 41.48, 91.66
α, β, γ (°)	90.00, 90.00, 90.00	90.00, 90.00, 90.00
Resolution (Å)	45.86 – 1.76 (1.79 – 1.76)	27.13 – 1.80 (1.83 – 1.80)
R_{merge}	9.9 (10.6)	8.7 (9.8)
$I / \sigma I$	15.2 (6.8)	13.9 (7.0)
Completeness (%)	99.5 (93.8)	96.0 (39.8)
Redundancy	4.7 (2.1)	5.0 (1.3)
Structure Refinement		
No. reflections	14433	13753
R_{work} / R_{free}	15.15 / 20.10	16.06 / 19.91
No. atoms		
Protein	1358	1358
GDP / Mg	28 / 1	28 / 1
Water	199	282
Ligand	18	27
B-factors		
Protein	15.28	12.20
GDP / Mg	15.07 / 14.19	11.41 / 13.76
Water	26.44	22.13
Ligand	25.06	19.38
R.m.s. deviations		
Bond lengths (Å)	0.024	0.004
Bond angles (°)	2.057	0.829

Methods

Cloning, expression and purification

The gene encoding the GTPase domain (residues 1-169) of oncogenic mutant K-Ras (G12D) was synthesized with codon optimization for *E. coli* overexpression. A C118S mutation was introduced to increase the stability of the protein during the NMR experiments[1] and is present in all of the K-Ras proteins described here. The expression construct was designed to include the tobacco etch viral protease (TEV) recognition sequence at the 5' end. This construct was inserted into a donor vector (pDONR-221) and transferred by recombinational cloning into the pDEST-HisMBP vector for expressing a fusion protein[2]. (pDEST-His-MBP and TEV vector provided by Dr. David S. Waugh) The K-Ras protein was expressed in Rosetta 2 (DE3) *E.coli* strain by induction with 1 mM IPTG at a cell density corresponding to an absorbance of OD_{600}=1.0. Isotopically-labeled K-Ras was prepared in M9 minimal media containing 1.0 g/L $^{15}NH_4Cl$. The fusion protein was purified on a Ni-IDA (ProBond from Invitrogen) column. TEV protease was added at a 1:20 molar ratio, and the solution was incubated at 4°C overnight. The reaction mixture was applied to a Ni-NTA column, and the K-Ras protein was collected in the flow through and exchanged into a low salt buffer. Wild-type K-Ras and other K-Ras mutants were expressed and purified in similar fashion. The catalytic domain of human Sos (residues 564-1049) was inserted into a donor vector (pDONR-221) and transferred by recombinational cloning into the pDEST-544 vector for expressing a His_6-tagged fusion protein. The Sos protein was expressed in BL21-CodonPlus-RIL *E.coli* strain by induction with 0.2 mM IPTG at a cell density of OD_{600}=1.0. The protein was expressed at 18°C overnight and then was purified on a Ni-IDA (ProBond from Invitrogen) column. Purified proteins were concentrated with Amicon ultra centrifugal columns (Millipore) and flash frozen in liquid N_2 and stored at -80°C.

Fragment library

A proprietary collection of 11,000 small molecules "fragments" was built by acquiring compounds from ChemBridge, ChemDiv, and five other vendors. Compounds were chosen for purchase if they passed criteria related to the commonly used "Rule of Three" (MW ≤300, cLogP ≤3.0, no more than 3 hydrogen bond donors)[3], and no more than 4 rotatable bonds. The fragment library is chemically diverse representing more than 700 distinctive ring systems and contains compounds that are relatively water soluble, and are devoid of highly reactive functional groups. We also selected compounds that contained molecular motifs known from the literature or from prior experience to be preferred for binding to proteins[4] as well as fragments contained in known drug molecules[5,6]. In addition, compounds were synthesized in the lab to supplement this collection with molecules and ring systems that are not commercially available and/or not known in the chemical literature. All of these compounds were required to pass a filter designed to remove molecules containing reactive intermediates and functional groups that were either considered unstable, overly promiscuous, or known to cause poor solubility or other performance issues in assays. Finally, the compounds were manually examined by experienced medicinal chemists and cheminformatics specialists to remove any additional unfavorable compounds not identified in the protocols.

Fragment-based screen

Compound binding was detected using two-dimensional sensitivity-enhanced $^{1}H/^{15}N$- HSQC spectra collected on a Bruker DRX500 spectrometer equipped with a cryoprobe and a Bruker Sample Jet sample changer. Each sample contained 50 μM GDP-bound K-Ras (G12D) protein and 12 fragments at a concentration of 650 μM. Positive hits were deconvoluted by testing samples containing the individual ligands. All screening compound plates were generated and data tracked using the sample handling capabilities of the Vanderbilt Institute of Chemical Biology (VICB) High Throughput Screening (HTS)

Core facility. Screening data were processed using Bruker TOPSPIN and analyzed by comparing spectra with and without compounds. Dissociation constants were obtained for selected compounds in fast exchange by monitoring the chemical shift changes of resonances as a function of compound concentration using standard fitting software.

Protein Crystallization

GDP-bound K-Ras (G12D/C118S, G12V/C118S or C118S) protein was exchanged into crystallization buffer (20 mM HEPES, 150 mM NaCl pH 8.0) and concentrated to 40 mg/mL. Protein-ligand complexes were prepared by adding a concentrated DMSO stock solution of the ligand to a final ligand concentration of 10-15 mM. All crystallization experiments were set up using the Mosquito crystallization robot (TTP Labtech, Royston UK) or performed manually using either the sitting or hanging-drop vapor diffusion method at 18 °C. Apo GDP-bound K-Ras (G12D/C118S) crystallized under a condition containing 30% PEG4000, 0.2 M Li_2SO_4 and 0.1 M sodium phosphate pH 7.5. The K-Ras(C118S)/**2** complex was crystallized from 30% PEG8000, 0.2 M sodium acetate and 0.1 M MES pH 6.5. The K-Ras(C118S)/**4** complex was crystallized from 25% PEG1500, 0.1 M MMT pH 4. The K-Ras(C118S)/**5** complex was crystallized from 32% PEG1500 and 0.7% 1-butanol. The K-Ras(G12V/C118S)/**6** complex was crystallized from 28% PEG8000, 0.1 M sodium acetate pH 4.5 and 5% DMSO. Complexes containing compounds **13** crystallized from 28% PEG4000, 0.2 M NH_4Cl and 0.1 M MMT pH 4. Single crystals were obtained after multiple rounds of microseeding. Crystals containing compounds **4**, **6** and **13** were cryo-protected with 10% ethylene glycol for low temperature data collection.

X-ray Data Collection, Structure Solution, and Refinement

X-ray diffraction data were collected at 100K in the oscillation mode on single flash-cooled crystals using a Bruker-NoniusMicrostar rotating anode X-ray generator equipped with a Proteum PT 135 CCD area

detector. The instrument is located in the Biomolecular Crystallography Facility in the Vanderbilt University Center for Structural Biology. Data were processed with HKL-2000[7], and structures were determined by molecular replacement using the coordinates of H-Ras G-domain (residues 1-166; PDB Entry 1AGP). The program package CCP4[8] and Phenix[9] were employed for phasing and refinement, and model fitting was performed with COOT[10]. Data collection and restrained refinement statistics are summarized in Table 1. The refined models were validated with PROCHECK and Phenix.

Nucleotide Exchange Assay

Purified, recombinant GDP-bound K-Ras is added to a mixture of Sos and BODIPY-GTP. Bound GDP is exchanged for BODIPY-GTP, resulting in an increase in fluorescence with time. The reaction was performed as an association-dissociation experiment in which BODIPY-GTP first associates with K-Ras followed by a dissociation step in which excess unlabeled GTP outcompetes the analog returning fluorescence to baseline. The rate of nucleotide exchange was determined by fitting a single exponential decay function to the dissociation phase of the experiment. Reactions were performed under increasing concentrations of compound in a buffer containing 25 mM Tris (pH 7.5), 50 mM NaCl, 1 mM DTT, and 20 μM $MgCl_2$ with final component concentrations of 1 μM, 1 μM, 1 μM, and 200 μM for Ras, Sos, BODIPY-GTP and unlabeled GTP, respectively.

Compound synthesis

All NMR spectra were recorded on a 400 MHz AMX Bruker NMR spectrometer. ^{1}H chemical shifts are reported in δ values in ppm with the deuterated solvent as the internal standard. Data are reported as follows: chemical shift, multiplicity (s = singlet, d = doublet, t = triplet, q = quartet, br = broad, m = multiplet), coupling constant (Hz), integration. Low resolution mass spectra were obtained on an Agilent 1200 series 6140 mass spectrometer with electrospray ionization. High resolution mass spectra were recorded on a Waters Q-TOF API-US plus Acquity system with electrospray ionization. All compounds were ≥95% purity as analyzed by LCMS. Analytical HPLC was performed on an Agilent 1200 series with UV detection at 214 and 254 nm along with ELSD detection. LCMS parameters were as follows: Phenomenex-C18 Kinetex column, 50 x 2.1 mm, 2 min gradient, 5% (0.1% TFA/MeCN) / 95% (0.1% TFA/ H_2O) to 100% (0.1% TFA/MeCN). Preparative purification was performed on a Gilson HPLC (Phenomenex-C18, 100 x 30 mm, 10 min gradient, 5→95% MeCN/H_2O with 0.1% TFA) or by automated flash column chromatography (Isco, Inc. 100sg Combiflash). Microwave heating was accomplished using a Biotage Initiator. All reagents were purchased from Sigma-Aldrich and used without purification.

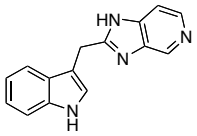

2-((1*H*-Indol-3-yl)methyl)-3*H*-imidazo[4,5-*c*]pyridine (4): A vial with a Teflon-coated septa was charged with carbonyldiimidazole (54 mg, 0.33 mmol), indole-3-acetic acid (53 mg, 0.30 mmol), and DMF (1 mL). 3,4-Diaminopyridine (36 mg, 0.33 mmol) was added in a single portion after 30 min of stirring at rt. The resulting red solution was then heated at 50 °C for 4 h. Concentration gave a brown residue that was dissolved in AcOH (1 mL) and heated at 180 °C for 2 h in a microwave reactor.

Purification of the concentrated residue by HPLC (5→95% MeCN/H_2O, 0.2% NH_4OH) gave a light brown solid (27 mg, 36%): ^{1}H NMR (400MHz, CD_3OD): δ 8.76 (s, 1H), 8.24 (d, J = 5.7 Hz, 1H), 7.49 (d, J = 5.6 Hz, 1H), 7.40 (d, J = 7.9 Hz, 1H), 7.36 (d, J = 8.2 Hz, 1H), 7.25 (s, 1H), 7.09 (t, J = 7.6 Hz, 1H), 6.96 (t, J = 5.7 Hz, 1H), 3.33 (s, 2H); LCMS: 0.60 min, *m/z* = 249 $[M+H]^+$; HRMS (*m/z*): $[M+H]^+$ calcd. for $C_{15}H_{13}N_4$: 249.1140; found 249.1142.

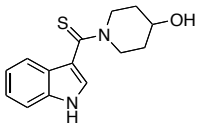

(4-Hydroxypiperidin-1-yl)(1*H*-indol-3-yl)methanethione (5): A slurry containing 72 mg (0.5 mmol) of indole-3-carbaldehyde, 51 mg (0.5 mmol) of 4-hydroxypiperidine, 19 mg (0.6 mmol) of sulfur, and 1.5 mL of DMF was heated in a microwave reactor at 120 °C for 10 min, and then 130 °C in a microwave reactor for an additional 5 min. The solvents were removed under reduced pressure and the residue was subjected to HPLC chromatography to give 53 mg (54%) of (4-hydroxypiperidin-1yl)(1*H*-indol-3-yl)methanethione as a yellow solid: ^{1}H NMR (400MHz, CD_3OD): δ 8.93 (brs, 1H), 7.81 (dd, *J* = 9.2, 5.6 Hz, 1H), 7.21 (d, *J* = 2.0 Hz, 1H), 7.13-7.11 (m, 1H), 7.02-6.99 (m, 2H), 3.88-3.85 (m, 1H), and 1.90-1.45 (brs, 5H); LCMS: 0.81 min, *m/z* = 261 $[M+H]^+$; HRMS (*m/z*): $[M+H]^+$ calcd. for $C_{14}H_{17}N_2OS$, 261.1062; found 261.1061.

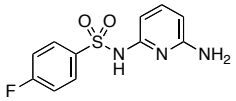

***N*-(6-aminopyridin-2-yl)-4-fluorobenzenesulfonamide (6).** To a solution of 2,6-diaminopyridine (110 mg, 1.0 mmol) in pyridine (1.5 mL) was added 4-fluorobenzne-1-sulfonyl chloride (100 mg, 0.5 mmol) dropwise at rt. The reaction mixture was stirred for 15 h and concentrated. The residue was purified by HPLC to give the product (100 mg, 74%) as a tan solid: ^{1}H NMR (400MHz, d_6-DMSO): δ 7.78-7.92 (m, 2H), 7.28-7.47 (m, 4H), 6.20-6.40 (br, 2H), 6.14 (d, *J* = 8.0 Hz, 1H), 5.92 (d, *J* = 8.1 Hz, 1H). LCMS:

0.78 min, *m/z* = 268 $[M+H]^+$; HRMS (*m/z*): $[M+H]^+$ calcd. for $C_{11}H_{11}N_3O_2FS$ 268.0556, found 268.0557.

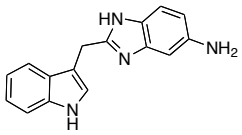

2-((1*H*-indol-3-yl)methyl)-1*H*-benzo[*d*]imidazol-5-amine (7). A flask was charged with carbonyldiimidazole (1.07 g, 6.6 mmol, 1.1 eq), indole-3-acetic acid (1.05 g, 6.0 mmol, 1 eq), and 1:1 THF/DMF (6 mL). 4-Nitro-o-phenylenediamine (1.01 g, 6.6 mmol) was added in a single portion after 30 min of stirring at rt. The resulting red solution was then heated at 50 °C for 12 h. Concentration gave a red residue that was dissolved in AcOH (6 mL) and heated at 120 °C for 30 min in a microwave reactor. The solution was concentrated, dissolved in EtOAc (12 mL), and 5% Pd-C (500 mg) was added. The mixture was allowed to stir under an atmosphere of H_2 for 8 h. Filtration through Celite and concentration gave a brown residue that was purified by HPLC to give a red solid (1.4 g, 89%): ^{1}H NMR (400MHz, CD_3OD): δ 8.37-8.32 (m, 1H), 8.07 (dd, *J* = 8.89, 2.20 Hz, 1H), 7.51 (d, *J* = 8.59 Hz, 1H), 7.38 (d, *J* = 7.95 Hz, 1H), 7.34 (d, *J* = 8.17 Hz, 1H), 7.23 (s, 1H), 7.07 (t, *J* = 7.19 Hz, 1H), 6.94 (t, *J* = 7.14 Hz, 1H), 4.40 (s, 2H); LCMS: 0.54 min, *m/z* = 263 $[M+H]^+$; HRMS (*m/z*): $[M+H]^+$ calcd. for $C_{16}H_{15}N_4$: 263.1297; found 263.1299.

General procedure for amide coupling. Aniline **7** (53 mg, 0.20 mmol, 1 eq), carboxylic acid (0.22 mmol, 1.1 eq), COMU ((1-Cyano-2-ethoxy-2-oxoethylidenaminooxy)dimethylamino-morpholino-carbenium hexafluorophosphate) (94 mg, 0.22 mmol, 1.1 eq), and iPr_2NEt (52 mg, 70 μL, 0.40 mmol, 2 eq) were dissolved in MeCN (1 mL) and allowed to stir at rt for 15 h. The resulting solution was concentrated and purified by HPLC. Amides containing Boc-protected amines were then removed using 1:1 TFA/CH_2Cl_2 (1 mL).

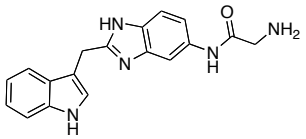

***N*-(2-((1*H*-indol-3-yl)methyl)-1*H*-benzo[*d*]imidazol-5-yl)-2-aminoacetamide (8).** Using the general procedure for amide coupling, a white solid (31 mg, 48%) was obtained: ^{1}H NMR (400MHz, CD_3OD): δ 7.89 (s, 2H), 7.41 (d, *J* = 8.0 Hz, 2H), 7.35 (d, *J* = 8.2 Hz, 1H), 7.25-7.18 (m, 2H), 7.08 (t, *J* = 7.6 Hz, 1H), 6.95 (t, *J* = 7.5 Hz, 1H), 4.35 (s, 1H), 3.41 (s, 2H); LCMS: 0.63 min, *m/z* = 320 $[M+H]^+$; HRMS (*m/z*): $[M+H]^+$ calcd. for $C_{18}H_{18}N_5O$: 320.1511; found 320.1509.

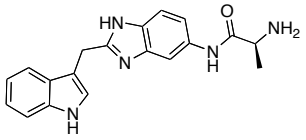

(*S*)-*N*-(2-((1*H*-indol-3-yl)methyl)-1*H*-benzo[*d*]imidazol-5-yl)-2-aminopropanamide (9). Using the general procedure for amide coupling, an ivory solid (27 mg, 41%) was obtained: ^{1}H NMR (400MHz, CD_3OD): δ 7.89 (d, *J* = 1.6 Hz, 1H), 7.41 (d, *J* = 7.9 Hz, 2H), 7.34 (d, *J* = 8.2 Hz, 1H), 7.23 (d, *J* = 8.4 Hz, 1H), 7.20 (s, 1H), 7.08 (t, *J* = 7.5 Hz, 1H), 6.94 (t, *J* = 7.5 Hz, 1H), 4.35 (s, 2H), 3.60-3.52 (m, 1H), 1.36 (d, *J* = 6.9 Hz, 3H); LCMS: 0.66 min, *m/z* = 334 $[M+H]^+$; HRMS (*m/z*): $[M+H]^+$ calcd. for $C_{19}H_{20}N_5O$: 334.1668; found 334.1669.

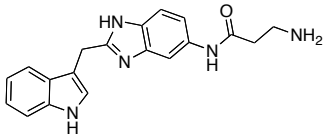

***N*-(2-((1*H*-indol-3-yl)methyl)-1*H*-benzo[*d*]imidazol-5-yl)-3-aminopropanamide (10).** Using the general procedure for amide coupling, a light yellow solid (30 mg, 46%) was obtained: ^{1}H NMR (400MHz, CD_3OD): δ 7.88 (d, *J* = 1.6 Hz, 1H), 7.44-7.38 (m, 2H), 7.35 (d, *J* = 8.2 Hz, 1H), 7.23-7.18 (m, 2H), 7.08 (t, *J* = 7.6 Hz, 1H), 6.95 (t, *J* = 7.5 Hz, 1H), 4.35 (s, 2H), 3.00 (t, *J* = 6.5 Hz, 2H), 2.56 (t, *J* = 6.5 Hz, 2H); LCMS: 0.69 min, *m/z* = 334 $[M+H]^+$; HRMS (*m/z*): $[M+H]^+$ calcd. for $C_{19}H_{20}N_5O$:

334.1668; found 334.1667.

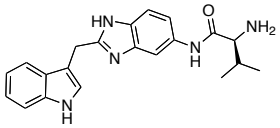

(*S*)-*N*-(2-((1*H*-indol-3-yl)methyl)-1*H*-benzo[*d*]imidazol-5-yl)-2-amino-3-methylbutanamide (11). Using the general procedure for amide coupling, a white solid (34 mg, 47%) was obtained:^{1}H NMR (400MHz, CD_3OD): δ 7.88 (d, *J* = 1.5 Hz, 1H), 7.41 (d, *J* = 7.9 Hz, 2H), 7.35 (d, *J* = 8.2 Hz, 1H), 7.25-7.19 (m, 2H), 7.08 (t, *J* = 7.5 Hz, 1H), 6.95 (t, *J* = 7.5 Hz, 1H), 4.36 (s, 2H), 3.23 (d, *J* = 5.8 Hz, 1H), 2.10-1.97 (m, 1H), 1.03 (d, *J* = 6.8 Hz, 3H), 0.99 (d, *J* = 6.8 Hz, 3H); LCMS: 0.75 min, *m/z* = 362 $[M+H]^+$; HRMS (*m/z*): $[M+H]^+$ calcd. for $C_{21}H_{24}N_5O$: 362.1981; found 362.1981.

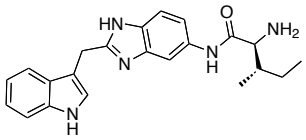

(2*S*,3*S*)-*N*-(2-((1*H*-indol-3-yl)methyl)-1*H*-benzo[*d*]imidazol-5-yl)-2-amino-3-methylpentanamide (12). Using the general procedure for amide coupling, a white solid (32 mg, 43%) was obtained:^{1}H NMR (400MHz, CD_3OD): δ 7.88 (d, *J* = 1.4 Hz, 1H), 7.41 (d, *J* = 7.9 Hz, 2H), 7.35 (d, *J* = 8.2 Hz, 1H), 7.27-7.18 (m, 2H), 7.08 (t, *J* = 7.5 Hz, 1H), 6.95 (t, *J* = 7.5 Hz, 1H), 4.36 (s, 2H), 1.79 (dtd, *J* = 9.8, 6.5, 3.8 Hz, 1H), 1.71-1.55 (m, 1H), 1.31-1.15 (m, 1H), 1.01 (d, *J* = 6.8 Hz, 3H), 0.94 (t, *J* = 7.4 Hz, 3H); LCMS: 0.79 min, *m/z* = 376 $[M+H]^+$; HRMS (*m/z*): $[M+H]^+$ calcd. for $C_{22}H_{26}N_5O$: 376.2137; found 376.2138.

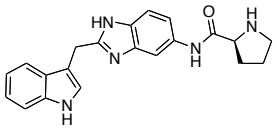

(*S*)-*N*-(2-((1*H*-indol-3-yl)methyl)-1*H*-benzo[*d*]imidazol-5-yl)pyrrolidine-2-carboxamide (13). Using the general procedure for amide coupling, a light brown solid (33 mg, 45%) was obtained: ^{1}H NMR

(400MHz, CD_3OD): δ 7.89 (d, *J* = 1.6 Hz, 1H), 7.45-7.38 (m, 2H), 7.34 (d, *J* = 8.2 Hz, 1H), 7.25-7.18 (m, 2H), 7.07 (t, *J* = 7.4 Hz, 1H), 6.94 (t, *J* = 7.5 Hz, 1H), 4.35 (s, 2H), 3.78 (dd, *J* = 8.7, 6.0 Hz, 1H), 3.06 (td, *J* = 10.6, 6.4 Hz, 1H), 2.96 (td, *J* = 10.5, 6.7 Hz, 1H), 2.27-2.15 (m, 1H), 1.94-1.75 (m, 3H); LCMS: 0.74 min, *m/z* = 360 $[M+H]^+$; HRMS (*m/z*): $[M+H]^+$ calcd. for $C_{22}H_{24}N_5O$: 374.1981; found 374.1983.

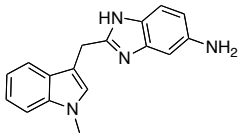

2-((1-methyl-1*H*-indol-3-yl)methyl)-1*H*-benzo[*d*]imidazol-5-amine (S1). A flask was charged with carbonyldiimidazole (178 mg, 1.1 mmol, 1.1 eq), 1-methyl-3-indoleacetic acid (189 g, 1.0 mmol, 1 eq), and 1:1 THF/DMF (2 mL). 4-Nitro-o-phenylenediamine (168 mg, 1.1 mmol, 1.1 eq) was added in a single portion after 30 min of stirring at rt. The resulting red solution was then heated at 50 °C for 12 h. Concentration gave a red residue that was dissolved in AcOH (2 mL) and heated at 120 °C for 3 h. The solution was concentrated, dissolved in EtOAc (5 mL), and 5% Pd-C (200 mg) was added. The mixture was allowed to stir under an atmosphere of H_2 for 5 h at 40 °C. Filtration and concentration gave a brown residue that was purified by HPLC to give a brown solid (173 mg, 62%): ^{1}H NMR (400MHz, CD_3OD): δ 7.46-7.36 (m, 3H), 7.31 (s, 1H), 7.23 (t, *J* = 7.6 Hz, 1H), 7.06 (t, *J* = 7.5 Hz, 1H), 7.00-6.94 (m, 2H), 4.59 (s, 2H), 3.85 (s, 3H); LCMS: 0.74 min, *m/z* = 277 $[M+H]^+$; HRMS (*m/z*): $[M+H]^+$ calcd. for $C_{17}H_{17}N_4$: 277.1453; found 277.1452.

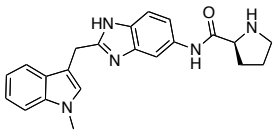

(*S*)-*N*-(2-((1-methyl-1*H*-indol-3-yl)methyl)-1*H*-benzo[*d*]imidazol-5-yl)pyrrolidine-2-carboxamide (S2). Using the general coupling procedure with aniline **S1**, a light brown solid (34 mg, 47%) was obtained: ^{1}H NMR (400MHz, CD_3OD): δ 7.89 (d, *J* = 1.4 Hz, 1H), 7.44-7.39 (m, 2H), 7.33 (d, *J* = 8.2 Hz, 1H), 7.22 (d, *J* = 7.9 Hz, 1H), 7.16 (d, *J* = 7.6 Hz, 1H), 7.12 (s, 1H), 6.98 (t, *J* = 7.5 Hz, 1H), 4.34 (s, 2H), 3.81-3.76 (m, 4H), 3.07 (td, *J* = 10.4, 6.4 Hz, 1H), 2.97 (td, *J* = 10.3, 6.7 Hz, 1H), 2.27-2.15 (m, 1H), 1.94-1.76 (m, 3H); LCMS: 0.80 min, *m/z* = 374 $[M+H]^+$; HRMS (*m/z*): $[M+H]^+$ calcd. for

$C_{21}H_{22}N_5O$: 360.1824; found 360.1823.

Accession codes. Protein Data Bank: the refined models and corresponding structure factor amplitudes will be deposited in the Research Collaboratory for Structural Biology (http://www.rcsb.org) under accession numbers 4EPV, 4EPW, 4EPT, 4EPX, 4EPR, and 4EPY.

References

1. Thapar, R., Williams, J.G. & Campbell, S.L. *J. Mol. Biol*. **343**, 1391-1408 (2004).

2. Nallamsetty, S., Austin, B.P., Penrose, K.J., & Waugh, D.S. *Protein Sci.* **14**, 2964-2971 (2005).

3. Congreve, M., Carr, R., Murray, C., Jhoti, H., *Drug Discov. Today.* **8**, 876-877 (2003).

4. Hajduk P.J., Bures, M., Praestgaard, J., & Fesik, S.W., *J. Med. Chem.* **43**, 3443–3447 (2000).

5. Bemis, G.W., Murcko, M.A., *J. Med. Chem*. **39**, 2887-2893 (1996).

6. Vieth, M., Siegel, M.G., Higgs, R.E., & Savin, K.A., *J. Med. Chem.* **47**, 224-232 (2004).

7. Otwinowski, Z. & Minor, W. *Methods Enzymol.* **276A,** 307-326 (1997).

8. Collaborative Computational Project, Number 4. *ActaCryst*. **D50**, 760-763 (1994).

9. Adams P.D., Grosse-Kunstleve R.W., Hung L.W. & Terwilliger T.C. *ActaCryst*. **D58**, 1948-1954 (2002).

10. Emsley, P., Lohkamp, B., Scott, W.G. & Cowtan, K. *ActaCryst*. **D66**, 486-501 (2010).